

RESEARCH

Open Access



Self-control study of multi-omics in identification of microenvironment characteristics in calcium oxalate kidney stones

Shang Xu¹, Zhi-Long Liu¹, Tian-Wei Zhang¹, Bin Li¹, Yuan-Chao Cao¹, Xin-Ning Wang^{1*} and Wei Jiao^{1*}

Abstract

Background Perform proteomic and metabolomic analysis on bilateral renal pelvis urine of patients with unilateral calcium oxalate kidney stones to identify the specific urinary microenvironment associated with stone formation.

Methods Using cystoscopy-guided insertion of ureteral catheters, bilateral renal pelvis urine samples are collected. Liquid chromatography-tandem mass spectrometry (LC-MS/MS) is employed to identify differential proteins and metabolites in the urine microenvironment. Differentially expressed proteins and differential metabolites are further analyzed for their biological functions and potential metabolic pathways through Gene Ontology (GO) analysis, Kyoto Encyclopedia of Genes and Genomes (KEGG) enrichment analysis, Reactome pathway analysis and Biomolecular Interaction Network Database protein-protein interaction (PPI) network analysis.

Results In the urine from the stone-affected side, 36 differential proteins were significantly upregulated, 4 differential proteins were downregulated, and 10 differential metabolites were significantly upregulated. Functional and pathway analyses indicate that the differentially expressed proteins are primarily involved in inflammatory pathways and complement and coagulation cascades, while the differential metabolites are mainly associated with oxidative stress.

Conclusion The proteomic and metabolomic profiles of the urinary microenvironment in stone-affected kidneys provide a more precise reflection of the pathophysiological mechanisms involved in stone formation and development.

Keywords Urolithiasis, Proteomics, Metabolomics, Urine, Liquid chromatography-tandem mass spectrometry

*Correspondence:

Xin-Ning Wang
wangxinning@qduhospital.cn
Wei Jiao

jiaowei@qduhospital.cn

¹Department of Urology, The Affiliated Hospital of Qingdao University, Qingdao, Shandong Province 266000, China



© The Author(s) 2025. **Open Access** This article is licensed under a Creative Commons Attribution-NonCommercial-NoDerivatives 4.0 International License, which permits any non-commercial use, sharing, distribution and reproduction in any medium or format, as long as you give appropriate credit to the original author(s) and the source, provide a link to the Creative Commons licence, and indicate if you modified the licensed material. You do not have permission under this licence to share adapted material derived from this article or parts of it. The images or other third party material in this article are included in the article's Creative Commons licence, unless indicated otherwise in a credit line to the material. If material is not included in the article's Creative Commons licence and your intended use is not permitted by statutory regulation or exceeds the permitted use, you will need to obtain permission directly from the copyright holder. To view a copy of this licence, visit <http://creativecommons.org/licenses/by-nc-nd/4.0/>.

Introduction

Urolithiasis is among the most common urologic diagnoses globally, with substantial burden and cost on health-care systems worldwide [1, 2]. It is estimated that 80% of kidney stones are composed of calcium oxalate and calcium phosphate, 10% of struvite, 9% of uric acid, and the remaining 1% consist of cystine or ammonium acid urate. Despite its ancient origins, the pathogenesis of urolithiasis remains incompletely understood [3]. Recent advancements in proteomic and metabolomic techniques have sparked new insights into the study of urolithiasis. These developments aim to: (1) provide effective tools for a deeper understanding of the mechanisms behind stone formation, and (2) assist in the discovery of novel biomarkers that could enhance the diagnosis, prevention, and treatment of urolithiasis [4, 5].

Urine, as a critical specimen, plays an essential role in exploring the composition and pathological and etiological factors in kidney stone disease [6, 7]. Previous studies have compared proteomic and metabolomic profiles in the urine of kidney stone patients and healthy individuals to identify differential proteins (DEPs) and differential metabolites (DMs) [8–12]. However, numerous factors—such as diet, gender, age, medication, physiological conditions, and even the timing of urine sample collection can profoundly impact the results. These variations add complexity and potential errors to multi-omic urine studies, thereby affecting the reliability of the findings [13]. Hence, using a self-controlled method could significantly reduce research errors.

A recent large cross-sectional study in China reported that approximately 4.9% of kidney stone cases are unilateral, representing about six-sevenths of all cases [14]. Clinically, it is common to see patients with recurrent stone formation in one kidney while the other kidney remains stone-free. This intriguing clinical observation not only raises important questions but also provides a valuable research opportunity. In this context, our study collected urine from the renal pelvises of patients with unilateral renal calcium oxalate stones. By applying proteomics and metabolomics, we aimed to examine the alterations in the urine microenvironment within the renal pelvis of these patients, thus gaining insights into the pathogenesis of kidney stones. Compared with previous studies, this research adopts an autologous control method for kidney - stone patients. It aims to discover the characteristics of the urine in the stone - containing renal pelvis of patients with unilateral calcium oxalate kidney stones, and to a certain extent, reveals the differences in the protein profiles and metabolic profiles of the bilateral renal pelvis urine of patients with unilateral kidney stones.

Materials and methods

Patients

From May 2023 to July 2023, a total of eight patients (7males and 1 female) diagnosed with unilateral kidney stones via Computed Tomography (CT) scan were recruited at the Affiliated Hospital of Qingdao University. Enrollment criteria included: (1) Age range of 18 to 80 years; (2) Presence of unilateral kidney stones, with a maximum stone diameter exceeding 1 cm on CT scans; (3) Postoperative stone analysis by infrared spectroscopy confirming the presence of calcium oxalate stones. Exclusion criteria were: (1) Patients with concurrent malignant tumors, hematologic disorders, metabolic diseases, or rheumatic immune diseases; (2) Individuals with urinary diversion methods in place, such as those who have undergone total cystectomy or kidney transplantation; (3) Patients with other renal pathologies, including renal tumors, previous kidney surgeries, solitary kidneys, renal malformations (e.g., horseshoe kidney, duplicated kidney), or acute and chronic renal diseases, including end-stage renal failure; (4) Those with severe urinary tract infections or a fever exceeding 37.5°C; (5) Patients experiencing urinary tract obstructions and hydronephrosis. We analyzed the composition of the stones using infrared spectroscopy. The sensitivity of this technique dictates that only components with a content exceeding 10% will be explicitly reported. The content of calcium oxalate in the stones exceeds 90%, making it the main component. If the content of other components is below 10%, they do not meet the reporting threshold.

All samples were collected prior to any medical or surgical intervention. Written informed consent for publication was obtained from each participant before sample collection. The study was conducted following ethical approval by the Bioethics Committee of the Affiliated Hospital of Qingdao University (Ethical number QYFY WZLL 28907) and abide by the Declaration of Helsinki principles.

Sample collection and preparation

Before the lithotripsy operation, 10 ml of urine was obtained from each renal pelvis after bilateral ureteral catheterization with F5 ureteral catheter through cystoscope (Fig. 1). The urine was centrifuged at 1000 rpm for 15 min and then stored at -80°C. Then the lithotripsy continues. 300 µL of 8 M urea was added to the sample and the protease inhibitor was added at 10% of the lysate. After centrifuging at 14,100×g for 20 min, the supernatant was collected. The protein concentration was determined using Bradford method, rest was frozen to -80°C.

Mass spectrometry conditions for urinary protein profile

For spectral library generation, samples were fractionated using a high pH reversed-phase fractionator. Mass

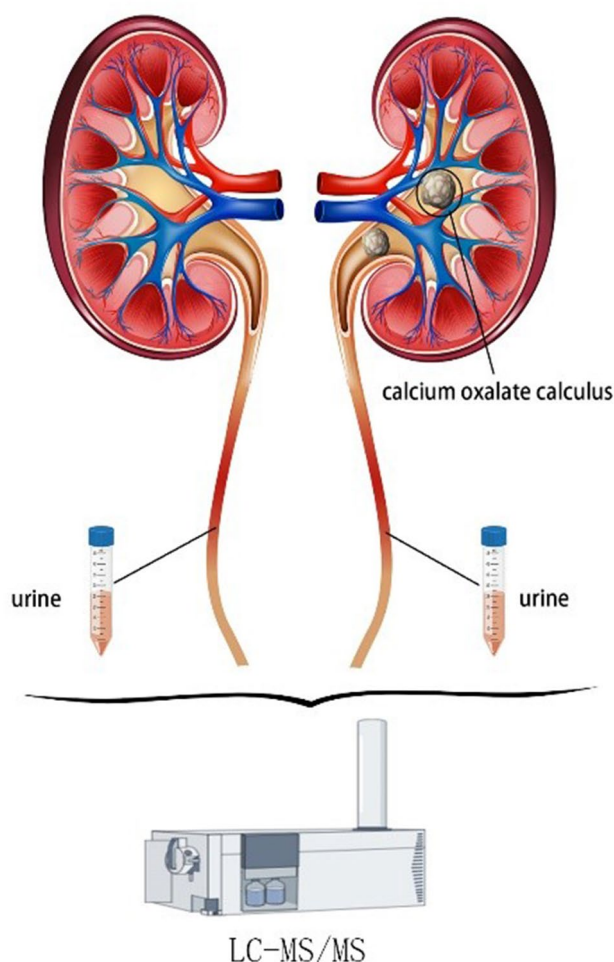


Fig. 1 Schematic representing the design of proteomics and metabolomics profiling experiments

spectrometry were subjected to liquid chromatography-tandem mass spectrometry (LC-MS/MS) using a 150 μ m I.D. 25 cm C18 column, 1.9 μ m particle size and a 80 min gradient: 8–95% solvent B (solvent A: 99.9% water, 0.1% formic acid; solvent B: 80% acetonitrile, 0.1% formic acid). The mass spectrometer was operated on a quadrupole Orbitrap mass spectrometer (Q Exactive HF-X, Thermo Fisher Scientific, Bremen, Germany) coupled to an EASY nLC 1200 ultra-high pressure system (Thermo Fisher Scientific) via a nano-electrospray ion source. Full details are provided in the Supplementary Material.

Data analysis of differentially expressed proteins (DEPs)

Gene Ontology (GO) was conducted using the interproscan-5 program against the non-redundant protein database, and the databases KEGG (Kyoto Encyclopedia of Genes and Genomes) was used to analyze the protein family and pathway. The probable interacting partners were predicted using the STRING-db server (<http://string.embl.de/>) based on the related species. STRING is a

database of both known and predicted protein-protein interactions [15]. We utilized Cytoscape v3.10.2 to create the protein-protein interaction (PPI) diagram. We annotated the pathways of DEPs in Reactome and conducted enrichment analysis. Reactome (<https://reactome.org>) is an open source, peer-reviewed biomolecular pathway knowledge database [16]. Upregulated proteins were set as having a fold change (FC) ≥ 1.5 , and downregulated proteins were set as having a FC ≤ 0.67 . The protein quantitative values in the comparisons were statistically analyzed using the paired T-test or Wilcoxon test, with a P-value of ≤ 0.05 considered as statistically significant.

Mass spectrometry conditions for urinary metabolic profile

Mass spectrometric detection of metabolites was performed on Orbitrap Exploris 120 (Thermo Fisher Scientific, USA) with ESI ion source. Simultaneous MS1 and MS/MS (Full MS-ddMS2 mode, data-dependent MS/MS) acquisition was used. The parameters were as follows: sheath gas pressure, 40 arb; aux gas flow, 10 arb; spray voltage, 3.50 kV and –2.50 kV for ESI(+) and ESI(-), respectively; capillary temperature, 325 $^{\circ}$ C; MS1 range, m/z 100–1000; MS1 resolving power, 60,000 full width at half maxima (FWHM); number of data dependant scans per cycle, 4; MS/MS resolving power, 15,000 FWHM; normalized collision energy, 30%; dynamic exclusion time, automatic.

Data analysis of metabolite and differential metabolites (DMs)

Upregulated metabolites were set as having a FC ≥ 1.2 , and downregulated proteins were set as having a FC ≤ 0.83 . The metabolites quantitative values in the comparisons were statistically analyzed using the paired T-test or Wilcoxon test, with a P-value of ≤ 0.05 considered as statistically significant. Finally, combined with P value and FC to screen biomarker metabolites. By default, when P value < 0.05 and FC > 1.2 or FC < 0.83 , we think that metabolite were considered to have significant differential expression. Differential metabolites were subjected to pathway analysis by MetaboAnalyst [17], which combines results from powerful pathway enrichment analysis with the pathway topology analysis. The identified metabolites in metabolomics were then mapped to the KEGG pathway for biological interpretation of higher-level systemic functions. The metabolites and corresponding pathways were visualized using KEGG Mapper tool.

Result

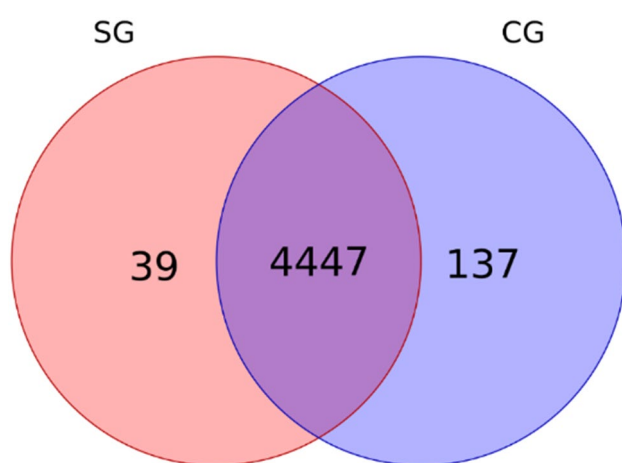
Demographic and clinical data of the studied subjects

This study included a total of 8 patients diagnosed with unilateral kidney stones. Bilateral renal pelvis urine was collected from these individuals. Detailed participant

Table 1 Demographic and clinical data of the studied subjects

Number	Age (y)	Gender	BMI (kg/m ²)	Plasma Cr (μmol/L)	Number of stone	Stone size (mm ²)	Hydronephrosis	Stone side	GFR(ml/min/1.73m ²)	CRP(mg/L)	WBC(10 ⁹ /L)
1	52	Male	26.6	74	Stag-horn	38×31	Mild	Left	100.81	<0.50	5.57
2	40	Male	19.5	67	1	15×6	Mild	Left	114.25	<0.50	6.31
3	58	Male	22.7	85	1	20×14	None	Right	98.61	<0.50	5.76
4	58	Male	22.9	56	1	25×15	Mild	Right	108.38	<0.50	3.66
5	31	Female	25.4	53	1	20×15	None	Left	121.49	<0.50	6.44
6	66	Male	23.9	68	3	32×18	Mild	Left	109.36	<0.50	5.63
7	44	Male	23.5	76	Multiple	20×25	Severe	Right	96.6	<0.50	5.03
8	42	Male	24.5	78	1	10×8	None	Left	105.48	<0.50	5.11

BMI, body mass index. Cr, Creatinine. GFR, glomerular filtration rate. CRP, C-reactive protein. WBC, white blood cell count

**Fig. 2** Number of proteins found in stone group (SG) and control group (CG)

demographics and clinical characteristics are presented in Table 1. All analyzed stones primarily consisted of calcium oxalate.

Proteomic analysis of urine samples

A total of 4623 proteins were identified by LC-MS/MS analysis of bilateral renal pelvis urine from the eight patients. In this cohort, 4,584 proteins were detected in the control group and 4,486 in the stone group, as shown in Fig. 2. Utilizing criteria of $FC > 1.5$ or < 0.67 and a $P\text{-value} < 0.05$, we distinguished 40 differential proteins between the groups; 36 were up-regulated, and 4 were down-regulated, as detailed in Table 2.

GO analysis of deps

To explore the possible biological functions of dysregulation proteins, we used the interproscan-5 program against the non-redundant protein database. Results demonstrated that the most enriched GO terms are related to cellular component (extracellular exosome, extracellular space, extracellular region), biological process (innate immune response, antimicrobial humoral

immune response, defense response to fungus) and molecular function (signaling receptor binding, heparin binding) (Fig. 3).

KEGG pathway analysis of deps

The KEGG pathway enrichment analysis was conducted to identify the functions of DEPs. The results showed that DEPs in stone group compared with the control group were involved in 274 KEGG pathways. As shown in Fig. 4, the top ten significant pathways were as follows: Complement and coagulation cascades, Neutrophil extracellular trap formation, Staphylococcus aureus infection, coronavirus disease 2019 (COVID-19), Cholesterol metabolism, Vitamin digestion and absorption, Amoebiasis, Fructose and mannose metabolism, African trypanosomiasis, Leukocyte transendothelial migration. The complement and coagulation cascades pathway was the most representative pathway, including 8 DEPs, followed by the Neutrophil extracellular trap formation and Staphylococcus aureus infection, encompassing 6 and 5 DEPs, respectively.

Reactome pathway analysis of deps

Reactome enrichment analysis demonstrated 108 pathways in DEPs. As shown in Fig. 5, the top five significant pathways were as follows: Regulation of TLR by endogenous ligand, MyD88 deficiency (TLR2/4), IRAK4 deficiency (TLR2/4), MyD88:MAL(TIRAP) cascade initiated on plasma membrane, Common Pathway of Fibrin Clot Formation.

Protein–protein interaction network of differentially expressed proteins

To further uncover the regulatory role of DEPs in Calculi - side renal pelvis urine and non - calculi - side renal pelvis urine, interactions between any set of two DEPs in this study were used to build a regulatory network using STRING and Cytoscape (Fig. 6). The results demonstrated that the DEPs constructed a complicated regulatory network containing 38 nodes and 92

Table 2 List of deps in the urine of bilateral renal pelvis in patients with unilateral kidney stones

Protein name	Abbreviation	Accession	Mean FC	P-value	Function	Expression
Neutrophil defensin 1	DEFA1B	P59665	97.85	0.012	Antibiotic	Up
Galectin-10	CLC	Q05315	61.58	0.012	Lectin	Up
Eosinophil cationic protein	RNASE3	P12724	54.25	0.012	Antibiotic	Up
Protein S100-A9	S100A9	P06702	37.71	0.012	Antimicrobial, Antioxidant	Up
Protein S100-A8	S100A8	P05109	30.64	0.028	Antimicrobial	Up
Coronin-1 A	CORO1A	P31146	29.73	0.038	Actin-binding	Up
Histone H1.5	H1-5	P16401	26.51	0.009	Receptor, Transducer	Up
Apolipoprotein B-100	APOB	P04114	23.70	0.018	Heparin-binding	Up
C4b-binding protein alpha chain	C4BPA	P04003	23.38	0.016	complement activation	Up
Integrin beta-2	ITGB2	P05107	17.31	0.026	Integrin, Receptor	Up
Neutrophil defensin 3	DEFA3	P59666	16.56	0.012	Antibiotic	Up
Plastin-2	LCP1	P13796	15.75	0.004	DNA-binding	Up
Fibrinogen beta chain	FGB	P02675	14.68	0.043	Blood coagulation	Up
Ras-related C3 botulinum toxin substrate 2	RAC2	P15153	14.48	0.041	Ligand	Up
Immunoglobulin heavy constant gamma 1	IGHG1	P01857	13.34	0.044	Adaptive immunity	Up
Apolipoprotein A-I	APOA1	P02647	13.28	0.032	Lipid metabolism	Up
Fascin	FSCN1	Q16658	13.06	0.012	Actin-binding	Up
Fibrinogen gamma chain	FGG	P02679	12.08	0.041	Blood coagulation	Up
Lamin-B1	LMNB1	P20700	12.05	0.030	Intermediate filament	Up
Apolipoprotein A-II	APOA2	P02652	11.64	0.030	Lipid transport	Up
Complement factor H	CFH	P08603	11.51	0.014	Complement alternate pathway	Up
Coagulation factor XIII B chain	F13B	P05160	10.98	0.045	Blood coagulation	Up
Phosphatidylinositol-glycan-specific phospholipase D	GPLD1	P80108	10.84	0.014	Hydrolase	Up
Histidine-rich glycoprotein	HRG	P04196	9.60	0.017	Heparin-binding	Up
Complement component C8 alpha chain	C8A	P07357	8.01	0.011	Translocase	Up
Fibrinogen alpha chain	FGA	P02671	7.35	0.012	Blood coagulation	Up
High mobility group protein B2	HMGB2	P26583	6.19	0.024	DNA-binding	Up
RNA-binding protein Raly	RALY	Q9UKM9	4.92	0.004	Ribonucleoprotein, RNA-binding	Up
Calponin-2	CNN2	Q99439	4.68	0.008	Actin-binding, Calmodulin-binding	Up
Aldo-keto reductase family 1 member B10	AKR1B10	O60218	4.29	0.017	Oxidoreductase	Up
Protein S100-A2	S100A2	P29034	4.13	0.024	Ligand	Up
Immunoglobulin lambda variable 6-57	IGLV6-57	P01721	3.69	0.012	Adaptive immunity	Up
Actin, alpha skeletal muscle	ACTA1	P68133	3.31	0.001	Hydrolase, Muscle protein	Up
Protein kinase C beta type	PRKCB	P05771	3.26	0.000	Kinase, Transferase	Up
Glucose-6-phosphate 1-dehydrogenase	G6PD	P11413	3.08	0.021	Oxidoreductase	Up
EH domain-binding protein 1-like protein 1	EHBP1L1	Q8N3D4	2.43	0.010	Unknown	Up
Testican-1	SPOCK1	Q08629	0.54	0.014	Unknown	Down
Bile salt-activated lipase	CEL	P19835	0.52	0.002	Hydrolase, Serine esterase	Down
GDP-mannose 4,6 dehydratase	GMDS	O60547	0.31	0.008	Lyase	Down
Uridine phosphorylase 1	UPP1	Q16831	0.23	0.004	Glycosyltransferase	Down

FC, Fold change

edges. Fibrinogen alpha chain and Fibrinogen gamma chain were the most important hubs interacting with 13 proteins.

Metabolomics analysis of urine samples

A total of 323 metabolites were detected, identified and quantified in 8 pairs of stone pelvis urine and healthy

kidney urine. We applied a dual criterion of $P < 0.05$ and $FC > 1.2$ to detect common features in eight paired samples, leading to the identification of 10 upregulated DMs (Table 3). Urinary metabolomics indicated that Adenosine and N7-Methylguanosine were significantly up-regulated in the urine of the kidney on the calculous side, and the FC was 12.15 and 10.36, respectively. In addition,

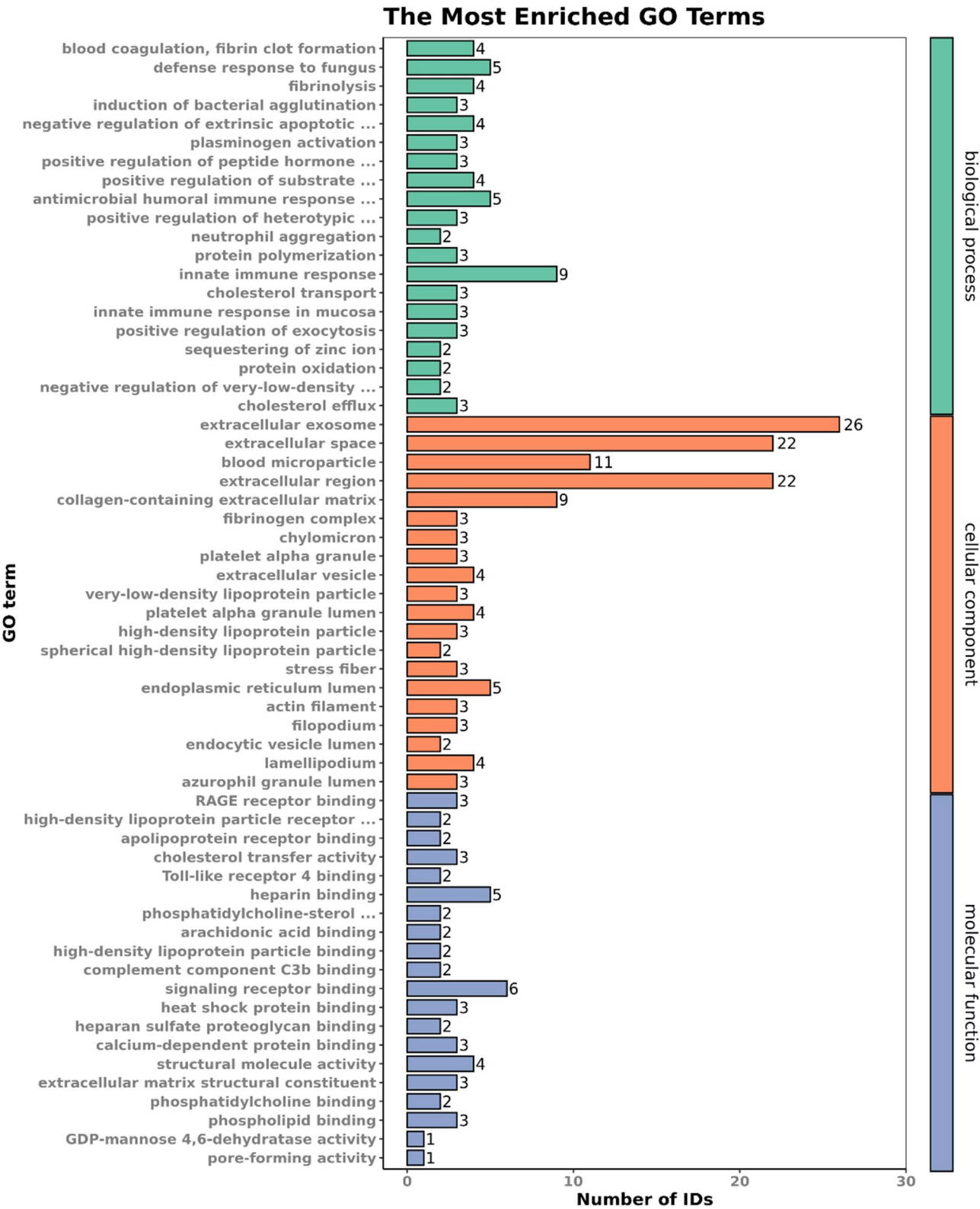


Fig. 3 GO analysis of the 40 DEPs for functional classification. Green, yellow and blue bars represent biological processes, cellular components, and molecular functions, respectively. The horizontal axis represents the number of DEPs

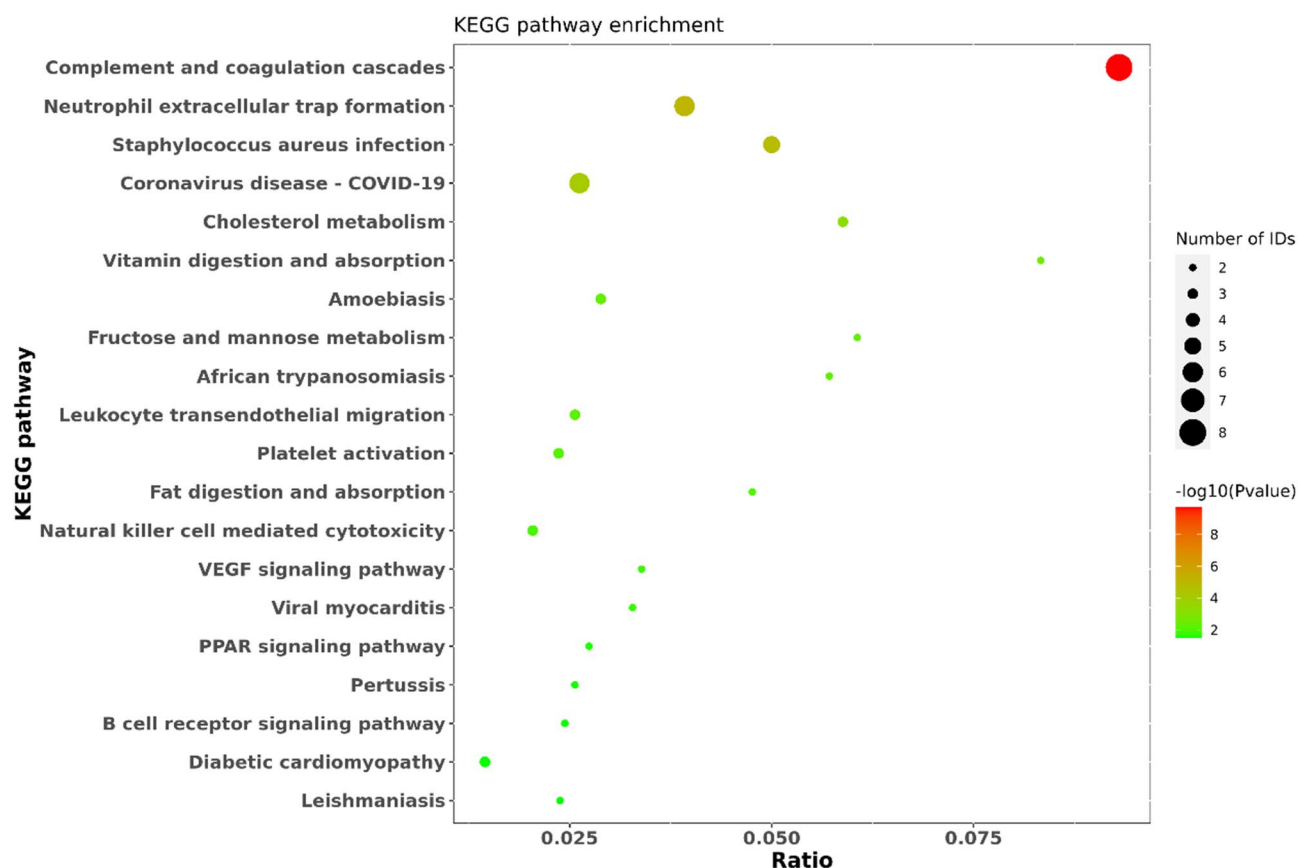


Fig. 4 KEGG pathway enrichment analysis of DEPs with the ten highest enrichment scores. The left y-axis shows the pathways. The right y-axis colored with gradient color is $-\log(P \text{ value})$ showing the enrichment score. The greater the enrichment score, the smaller the P value, signifying the significant enrichment of DEPs within the specified pathways

eight different metabolites were significantly upregulated in the lithic side samples, namely Methylmalonic acid, 2-Phenylacetamide, 4-Guanidinobutanoic acid, Acetaminophen, 2-Amino-3-phosphonopropionic acid, 3-Hydroxyanthranilic acid, 8-Methoxykynurenate and 3-Hydroxykynurenine.

KEGG pathway analysis of of dysregulated metabolites

The KEGG analysis shows that dysregulated metabolites were enriched in Tryptophan metabolism, GMP-PKG signaling pathway, Alcoholism, Morphine addiction (Fig. 7). The Tryptophan metabolism pathway was the most representative pathway.

Discussion

The pathogenesis of urinary calculi is complex and remains an unresolved global health issue [18]. Proteomic and metabolomic profiling of urine shows promising potential in diagnosing and treating kidney diseases. However, the majority of existing research primarily contrasts the urine composition between individuals with kidney stones and those without, without delving into comprehensive multi-omics investigations of the

bilateral renal pelvis urine in patients with unilateral kidney stones. Urine is inherently unstable and varies greatly due to factors such as diet, gender, age, medications, and even the timing of urine collection. These variables introduce significant complexity and potential errors in multi-omics studies of urine, impacting the reliability of the results [4]. In our study, we collected urine directly from the renal pelvis of patients with unilateral kidney stones using ureteral catheterization. This autologous control approach allows for a more efficient and accurate evaluation of the urinary microenvironment where stone formation occurs. However, inserting the ureteral catheter inevitably exerts certain mechanical stimulation on the ureteral tissue. This kind of stimulation may trigger a stress response in the local tissue, leading to an increase in the release of some endogenous proteins or metabolites. These additional substances generated by the stimulation may mask the changes in proteins and metabolites originally present in the sample that are related to the research purpose, or interfere with their accurate detection. We have maximally removed cell debris and impurities from the samples during the pre-treatment process to ensure the stability of the urine samples. During the

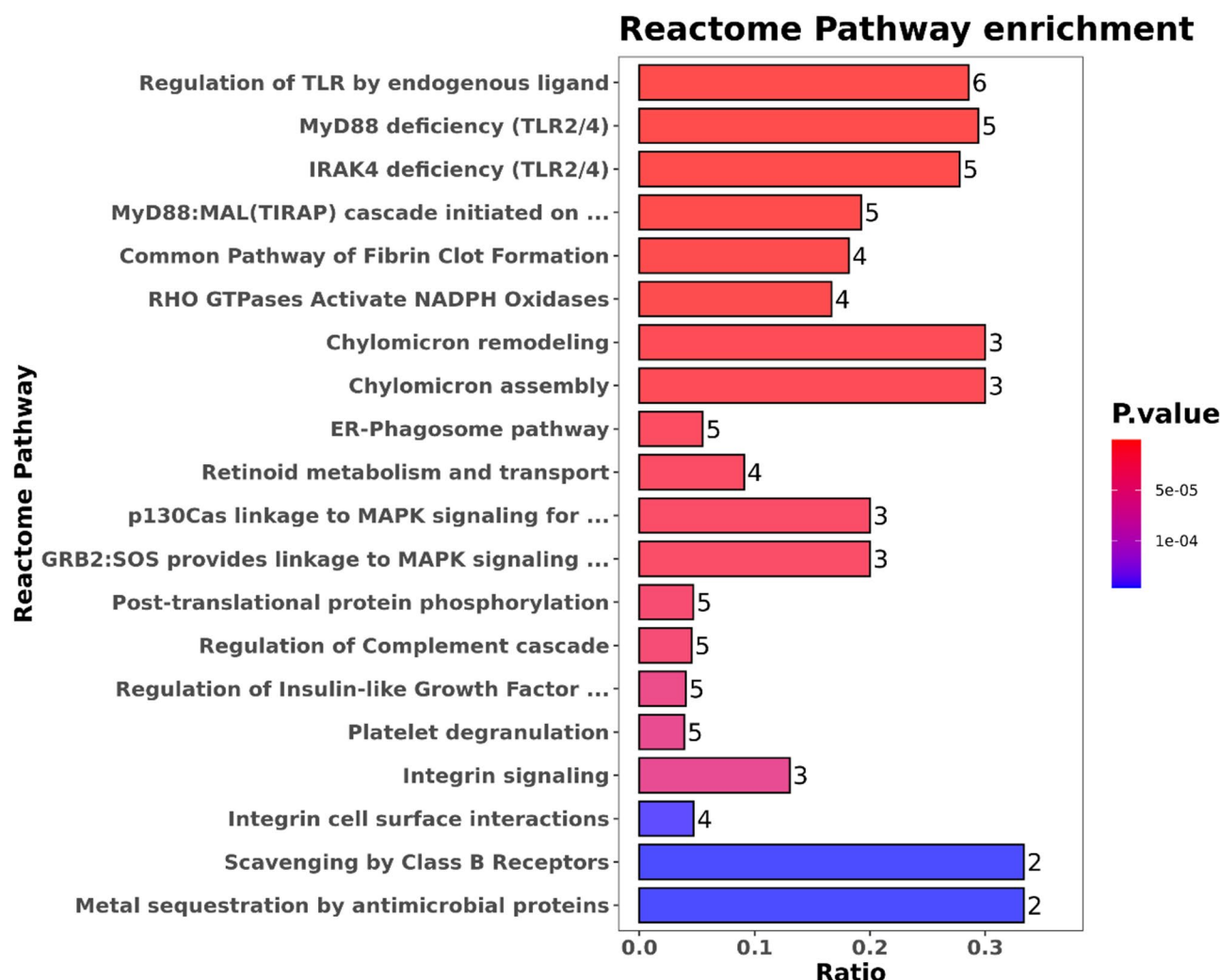


Fig. 5 Reactome pathway enrichment analysis of DEPs with the ten highest enrichment scores. The left y-axis shows the pathways. The right y-axis colored with gradient color is P value showing the enrichment score

pre - treatment of samples, we've made every effort to remove cell debris and impurities from the samples, ensuring the stability of the urine samples. However, collecting urine via a ureteral catheter may still have some potential impacts that can't be completely avoided.

By performing quantitative analysis, P value < 0.05 and FC > 1.5 as the screening criterion, a total of 40 proteins with significant differences were identified (36 up-regulated and 4 down-regulated). The most highly upregulated protein was Neutrophil defensin 1, with a mean FC of 97.85, followed by Galectin-10, Eosinophil cationic protein, Protein S100A9, and Protein S100A8, each displaying an average FC above 30. The most notably downregulated protein was Testican-1, followed by Bile salt-activated lipase.

Neutrophil defensin 1 is a key component of the innate immune system with broad-spectrum antimicrobial effects against bacteria, fungi, and other pathogens

[19]. S100 calcium binding protein A8 (S100A8) and A9 (S100A9) belong to the S100 family of calcium-binding proteins, which are primarily secreted by neutrophils and plays a prominent role in the regulation of inflammatory processes and immune response [20]. Research shows that S100A8 and S100A9 are the most abundant components in the matrix of kidney stones, and their expression is significantly increased in the renal tissues of patients with urolithiasis [21]. Our study revealed that in the urinary microenvironment where kidney stones exist, the levels of S100A8 and S100A9 were significantly elevated, exceeding 30 times the levels found in urine without stones. This suggests that both S100A8 and S100A9 play a crucial role in the formation and progression of kidney stones. The eosinophil cationic protein is a small polypeptide that originates from activated eosinophil granulocytes and exhibits antibacterial activity [22]. Galectin-10 also known as Charcot-Leyden

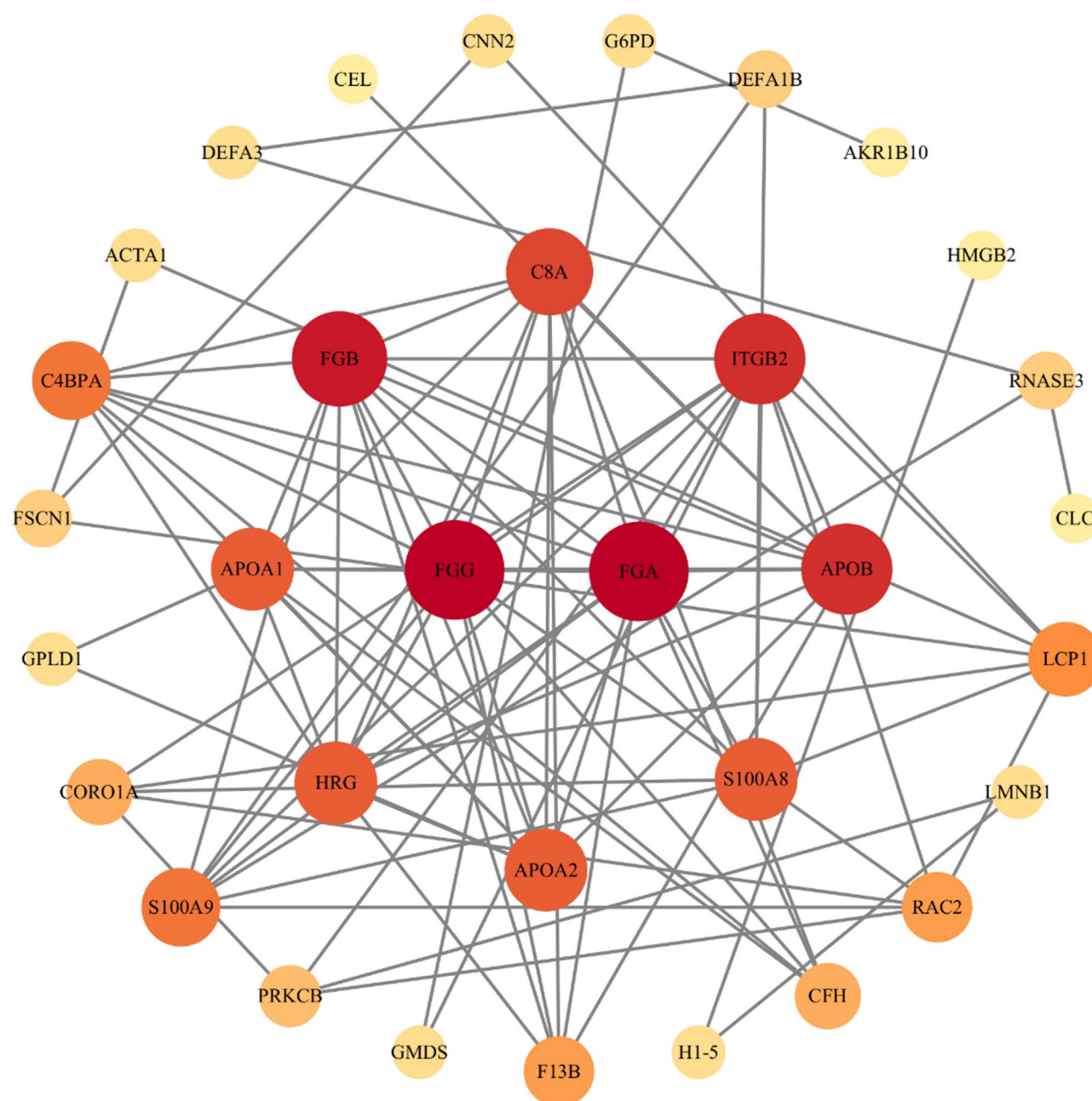


Fig. 6 Protein-protein interaction networks of the DEPs. PPI analysis was based on fold changes of protein expression. The gray colored lines represent interactions between proteins and proteins

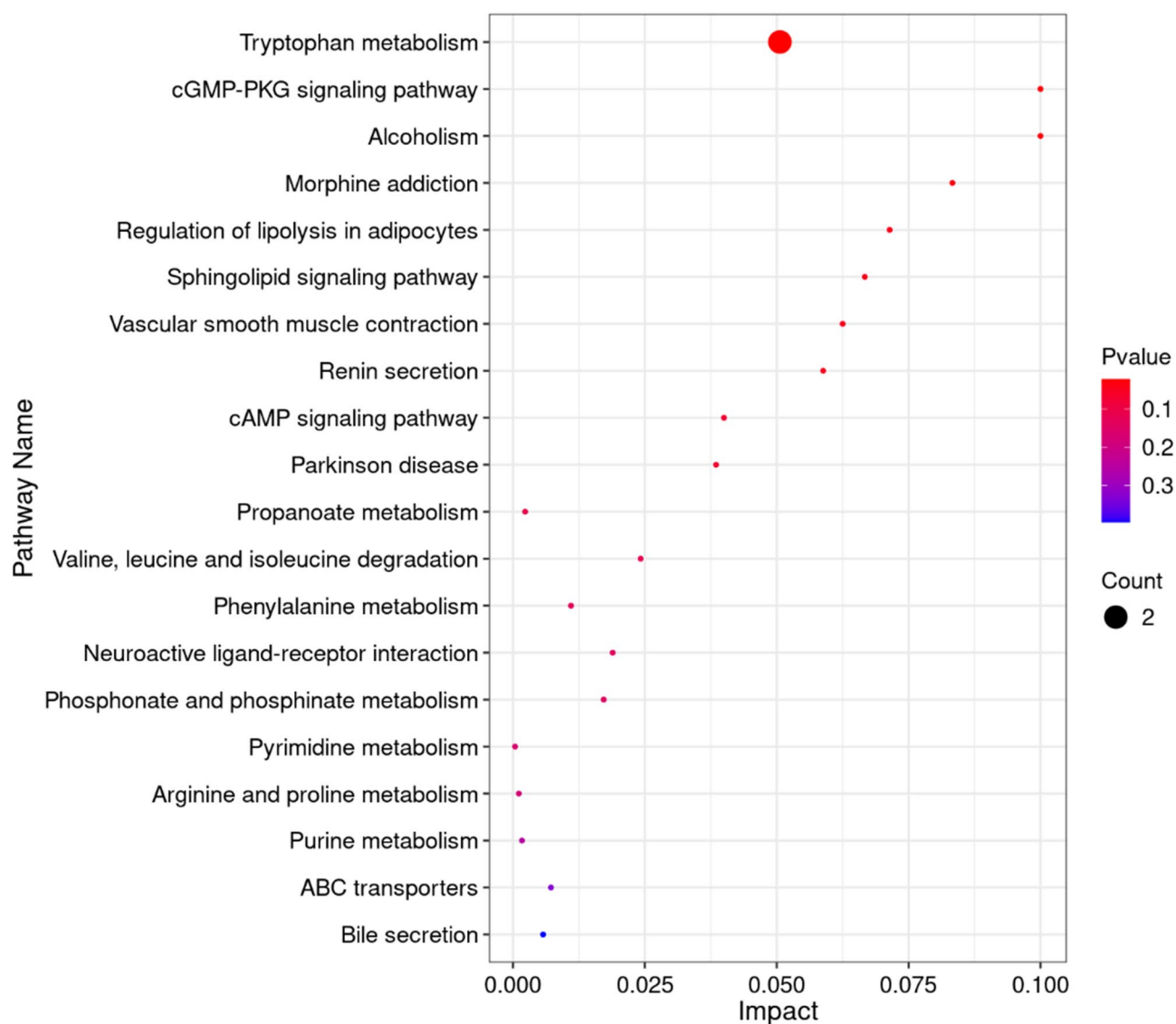
crystal protein, is highly expressed in human eosinophils and considered a biomarker of eosinophil involvement in inflammation [23]. Eosinophilic cationic proteins and neutrophil defense protein-1 were also found to be common components of the stone matrices [24, 25]. Thus, the findings indicate that inflammatory responses within the urinary microenvironment, particularly those involving neutrophils and eosinophils, play an essential role in the pathophysiology of kidney stone formation.

It is plausible to observe an elevation in blood microparticles within the urinary microenvironment in the presence of stones. Components like fibrinogen and clotting factors are likely to be increased due to the inherent damage caused by stone. This damage typically induces minor bleeding and initiates a coagulation cascade, contributing to the presence of these microparticles. We also noted that urine apolipoprotein levels were elevated in the stone group, suggesting a possible disturbance in lipid metabolism. Similarly, GO analysis revealed that

Table 3 List of DMs in the urine of bilateral renal pelvis in patients with unilateral kidney stones

Name	Mz	Formula	KEGG	p-value	Mean FC
Adenosine	268.1046	C ₁₀ H ₁₃ N ₅ O ₄	C00212	0.001	12.15
N7-Methylguanosine	298.1151	C ₁₁ H ₁₆ N ₅ O ₅	C20674	0.018	10.36
3-Hydroxykynurenine	224.1247	C ₁₀ H ₁₂ N ₂ O ₄	C02794	0.004	2.83
8-Methoxykynurenate	219.0477	C ₁₁ H ₉ NO ₄	C05830	0.003	2.13
3-Hydroxyanthranilic acid	154.0503	C ₇ H ₇ NO ₃	C00632	0.001	2.13
4-Guanidinobutanoic acid	146.0818	C ₅ H ₁₁ N ₃ O ₂	C01035	0.002	2.12
Methylmalonic acid	101.0717	C ₄ H ₆ O ₄	C02170	0.003	2.07
2-Phenylacetamide	136.0762	C ₈ H ₉ NO	C02505	0.040	2.05
2-Amino-3-phosphonopropionic acid	152.0098	C ₃ H ₈ N ₂ O ₅ P	C05672	0.000	2.05
Acetaminophen	151.062	C ₈ H ₉ NO ₂	C06804	0.001	2.03

Mz, mass-to-charge ratio. FC, Fold change

**Fig. 7** KEGG pathway enrichment analysis of DMs with the ten highest enrichment scores

most DEPs are mainly extracellular exosome and infection-related proteins. The KEGG analysis also suggested that the renal pelvis urine on the calculus side was mainly composed of coagulation cascade pathways, anti-infection-related pathways and cholesterol metabolism.

Previous research has indicated that the renal stones can stimulate tubular epithelial and immune cells to secrete inducible chemokines via TLR4 (Toll-like receptor 4) pathway and TLR2 (Toll-like receptor 2) pathway. This activation initiates a “chemokine to cytokine to chemokine” cascade, which may play a crucial role in urolithiasis pathogenesis. In concordance with these findings, our study has arrived at comparable conclusions. The data presented in Fig. 6 illustrate that that DEPs in the urine microenvironment are significantly enriched in the endogenous ligand-regulated TLR pathway.

For DMs, we investigated the potential metabolic pathways of metabolic alterations through the KEGG database and found that Tryptophan metabolism, cGMP-PKG signaling pathway, Alcoholism, Morphine addiction are involved in the formation of kidney stones. Adenosine and 7-Methylguanine were found to be significantly more than 10-fold higher in the urine collected from the calculus (stone-containing) side compared to the urine from the non-calculus side. This observation led us to hypothesize that the elevated levels of these compounds were likely due to cell death or injury. When cells are damaged or undergoing cell death, their internal components, including nucleosides, may be released into the surrounding fluid, such as urine. Furthermore, both adenosine and 7-Methylguanine are known to be involved in physiological processes such as immune response and inflammation [26, 27].

3-Hydroxyanthranilic acid, 8-Methoxykynurenate and 3-Hydroxykynurenine are related products in the kynurenine pathway of tryptophan metabolism. In the human body, kynurenate metabolites regulate biological processes including host microbiome signaling, immune cell responses, and neuronal excitability [28]. 8-Methoxykynurenate has been found to be enriched in COVID-19 patients. 3-Hydroxykynurenine and 3-Hydroxyanthranilic acid have been shown to have pro-oxidation activities, which can induce oxidative stress through the production of free radicals [29]. Additionally, the kynurenine pathway of tryptophan metabolism can produce Nicotinamide adenine dinucleotide (NAD⁺), which is a coenzyme involved in many cellular oxidation-reduction reactions [30].

Methylmalonic acid is an important intermediate in carbohydrate and amino acid metabolism in the human body. Studies have suggested that it may act as an endogenous neurotoxin, causing dilation of renal tubules, swelling of mitochondrial tubular epithelia and disorganization of cristae, which in turn leads to renal tubular

damage [31, 32]. 4-Guanidinobutyric acid, an alkaloid included in guanidino compounds, has stimulatory effects on monocytes and granulocytes, and oxidative burst activity has been observed in granulocytes [33]. Levillain, O et al. believe that the specific accumulation of toxic guanidino compounds in the injured kidney reflects disturbances in renal metabolism and function [34]. Hydroquinone and Acetaminophen are the major metabolite of aniline, which is an important intermediate in the dye industry. Acetaminophen is considered a well-known and widely used analgesic and antipyretic drug. In some cases, it can cause nephrotoxicity through oxidative stress. Research suggests that acetaminophen may cause renal tubular damage via pathways such as the enhancement of TNF- α levels, elevation in nitric oxide production, involvement in oxidative-nitrosative stress, and reduction in Na⁺/K⁺-ATPase activity [35–37]. This kind of tubular damage may lead to increased adhesiveness of calcium oxalate crystals, thereby promoting the aggregation of stones [38]. Researches have shown that Hydroquinone can trigger pyroptosis and endoplasmic reticulum stress through Ahr-regulated human lymphocyte oxidative stress [39]. Furthermore, it has been proved that it has a unique antibacterial mechanism against *Staphylococcus aureus* [40].

We have found that the majority of DMs are associated with oxidative stress, which has also been confirmed by previous studies [41]. This may suggest that not only is there an increase in oxidative stress products in the kidneys of patients with stones, but even the urinary microenvironment of the two kidneys (stone-bearing and non-stone-bearing) within the same individual can exhibit significant differences.

This study has several limitations. First, it didn't explore the DEPs and DMs in the urine of healthy individuals and kidney stone patients. Second, the sample size is small. The determination of unilateral kidney stones relied only on patients' CT scan images and medical histories, unable to guarantee the contralateral kidney is stone-free. Also, infrared spectral analysis of kidney stones can't ensure the calcium oxalate stone component in the sample exceeds 99%. Lack of follow-up research on postoperative patients makes it difficult to clarify whether these differences emerged after kidney stone formation or existed beforehand. Thus, it's hard to tell whether inflammation and oxidative stress cause kidney stone formation or are the results.

Conclusion

Our study found that even in patients with unilateral renal stones, significant differences exist in the proteins and metabolites in the renal pelvis urine of both kidneys. These DEPs and DMs primarily play a crucial role in the

development and progression of renal stones through inflammatory responses and oxidative stress.

Supplementary Information

The online version contains supplementary material available at <https://doi.org/10.1186/s12882-025-04026-1>.

Supplementary Material 1

Acknowledgements

The authors declare no acknowledgment.

Author contributions

SX reviewed the literature and contributed to manuscript drafting. TZ, BL and ZL collected and summarize data. SX and YC analyzed the data. XW and WJ were responsible for the revision of the manuscript for important intellectual content. All authors listed have made a substantial, direct, and intellectual contribution to the work and approved it for publication.

Funding

This research was supported by the Shandong Province medical health science and technology project (NO.202304051690).

Data availability

The datasets used and/or analysed during the current study are available from the corresponding author on reasonable request.

Declarations

Ethics approval and consent to participate

The study was conducted following ethical approval by the Bioethics Committee of the Affiliated Hospital of Qingdao University (Ethical number QYFY WZLL 28907) and abide by the Declaration of Helsinki principles. All participants in the study provided informed consent and signed the informed consent form.

Consent for publication

Not applicable.

Competing interests

The authors declare no competing interests.

Received: 30 June 2024 / Accepted: 19 February 2025

Published online: 27 February 2025

References

- Lang J, et al. Global trends in incidence and burden of urolithiasis from 1990 to 2019: an analysis of global burden of disease study data. *Eur Urol Open Sci*. 2022;35:37–46.
- Tundo G, et al. Beyond prevalence: annual cumulative incidence of kidney stones in the united States. *J Urol*. 2021;205(6):1704–9.
- Coe FL, Evan A, Worcester E. Kidney stone disease. *J Clin Invest*. 2005;115(10):2598–608.
- González-Buitrago JM, Ferreira L, Lorenzo I. Urinary proteomics. *Clin Chim Acta*. 2007;375(1–2):49–56.
- Kowalczyk NS, Prochaska ML, Worcester EM. Metabolomic profiles and pathogenesis of nephrolithiasis. *Curr Opin Nephrol Hypertens*. 2023;32(5):490–5.
- Sui W, Hsi RS. Linking 24-h urines to clinical phenotypes: what alternatives does the future bring? *Curr Opin Urol*. 2020;30(2):177–82.
- Khamis MM, Adamko DJ, El-Anead A. Mass spectrometric based approaches in urine metabolomics and biomarker discovery. *Mass Spectrom Rev*. 2017;36(2):115–34.
- Boonla C, et al. Inflammatory and fibrotic proteins proteomically identified as key protein constituents in urine and stone matrix of patients with kidney calculi. *Clin Chim Acta*. 2014;429:81–9.
- Thongprayoon C, et al. Nuclear magnetic resonance metabolomic profiling and urine chemistries in incident kidney stone formers compared with controls. *J Am Soc Nephrol*. 2022;33(11):2071–86.
- Duan X, et al. (1)H NMR-based metabolomic study of metabolic profiling for the urine of kidney stone patients. *Urolithiasis*. 2020;48(1):27–35.
- Xu ZJ, et al. Differential oral and gut microbial structure related to systemic metabolism in kidney stone patients. *World J Urol*. 2024;42(1):6.
- Wright CA, et al. Label-free quantitative proteomics reveals differentially regulated proteins influencing urolithiasis. *Mol Cell Proteom*. 2011;10(8):M110005686.
- Aitekenov S, Gaipov A, Bukasov R. Review: detection and quantification of proteins in human urine. *Talanta*. 2021;223(Pt 1):121718.
- Fan X, et al. Metabolic differences between unilateral and bilateral renal stones and their association with markers of kidney injury. *J Urol*. 2022;207(1):144–51.
- Szklarczyk D, et al. The STRING database in 2023: protein-protein association networks and functional enrichment analyses for any sequenced genome of interest. *Nucleic Acids Res*. 2023;51(D1):D638–46.
- Gillespie M, et al. The reactome pathway knowledgebase 2022. *Nucleic Acids Res*. 2022;50(D1):D687–92.
- Xia J, Wishart DS. Web-based inference of biological patterns, functions and pathways from metabolomic data using metaboanalyst. *Nat Protoc*. 2011;6(6):743–60.
- Wang Z et al. Recent advances on the mechanisms of kidney stone formation (Review). *Int J Mol Med*. 2021. 48(2).
- Erickson B, et al. Antibacterial activity and specificity of the six human [alpha]-defensins. *Antimicrob Agents Chemother*. 2005;49(1):269–75.
- Donato R, et al. Functions of S100 proteins. *Curr Mol Med*. 2013;13(1):24–57.
- Yang Y, et al. Proteomic analysis reveals some common proteins in the kidney stone matrix. *PeerJ*. 2021;9:e11872.
- de Oliveira PC, et al. Eosinophil cationic protein: overview of biological and genetic features. *DNA Cell Biol*. 2012;31(9):1442–6.
- Su J. A brief history of Charcot-Leyden crystal Protein/Galectin-10 research. *Molecules*. 2018. 23(11).
- Mushtaq S, et al. Identification of myeloperoxidase, alpha-defensin and Calgranulin in calcium oxalate renal stones. *Clin Chim Acta*. 2007;384(1–2):41–7.
- Chen WC, et al. Mass spectroscopic characteristics of low molecular weight proteins extracted from calcium oxalate stones: preliminary study. *J Clin Lab Anal*. 2008;22(1):77–85.
- Linden J, Koch-Nolte F, Dahl G. Purine release, metabolism, and signaling in the inflammatory response. *Annu Rev Immunol*. 2019;37:325–47.
- Yang L, Yuan L. Identification of novel N7-methylguanine-related gene signatures associated with ulcerative colitis and the association with biological therapy. *Inflamm Res*. 2023;72(12):2169–80.
- Cervenka I, Agudelo LZ, Ruas JL. Kynurenines: Tryptophan's metabolites in exercise, inflammation, and mental health. *Science*. 2017. 357(6349).
- Okuda S, et al. 3-Hydroxykynurenine, an endogenous oxidative stress generator, causes neuronal cell death with apoptotic features and region selectivity. *J Neurochem*. 1998;70(1):299–307.
- Minhas PS, et al. Macrophage de Novo NAD(+) synthesis specifies immune function in aging and inflammation. *Nat Immunol*. 2019;20(1):50–63.
- Kölker S, Okun JG. Methylmalonic acid—an endogenous toxin? *Cell Mol Life Sci*. 2005;62(6):621–4.
- Kashtan CE et al. Chronic Administration of Methylmalonic Acid (MMA) to Rats Causes Proteinuria and Renal Tubular Injury • 1815.
- Schepers E, et al. Guanidino compounds as cause of cardiovascular damage in chronic kidney disease: an in vitro evaluation. *Blood Purif*. 2010;30(4):277–87.
- Levillain O, et al. Influence of 72% injury in one kidney on several organs involved in Guanidino compound metabolism: a time course study. *Pflügers Arch*. 2001;442(4):558–69.
- Abdel-Zaher AO, et al. The potential protective role of alpha-lipoic acid against acetaminophen-induced hepatic and renal damage. *Toxicology*. 2008;243(3):261–70.
- Ghosh J, et al. Acetaminophen induced renal injury via oxidative stress and TNF-alpha production: therapeutic potential of Arjunolic acid. *Toxicology*. 2010;268(1–2):8–18.
- Das J, et al. Taurine protects acetaminophen-induced oxidative damage in mice kidney through APAP urinary excretion and CYP2E1 inactivation. *Toxicology*. 2010;269(1):24–34.
- Bet VV, et al. Depleted nitrite and enhanced oxidative stress in urolithiasis. *Indian J Clin Biochem*. 2006;21(2):177–80.

39. Yang X, et al. Hydroquinone triggers pyroptosis and Endoplasmic reticulum stress via AhR-regulated oxidative stress in human lymphocytes. *Toxicol Lett.* 2023;376:39–50.
40. Ma C, et al. Antimicrobial mechanism of hydroquinone. *Appl Biochem Biotechnol.* 2019;189(4):1291–303.
41. Wigner P et al. The molecular aspect of nephrolithiasis development. *Cells*, 2021. 10(8).

Publisher's note

Springer Nature remains neutral with regard to jurisdictional claims in published maps and institutional affiliations.